# Parabrachial PACAP Activation of Amygdala Endosomal Extracellular-Regulated Kinase Signaling Regulates the Emotional Component of Pain

## *Supplemental Information*

### Supplementary Methods and Materials

### Animals

Adult male Sprague-Dawley rats were from Charles River Laboratories, Wilmington, MA. PACAP promoter-dependent EGFP BAC transgenic mice, generated by the GENSAT (Gene Expression Nervous System Atlas) project were obtained from James Waschek (UCLA, Los Angeles, CA). The PACAP-EGFP mice have been described previously (1). In brief, the BAC contained 6.5 kb of the murine PACAP gene and approximately 97 kb 5' and 107 kb 3' flanking sequences; the BAC did not harbor other known genes. The EGFP-encoding cassette, tethered to a polyadenylation signal, was inserted downstream of the promoter region and upstream of the ATG Met initiation codon of PACAP. This design strategy prevented run-through expression of PACAP gene. The modified BAC transgene was linearized and injected into pronuclei of FVB/NTac mice by standard GENSAT protocols. An optimal founder was identified and mice regenerated from embryos were bred at UCLA vivarium. Breeding pairs for the PACAP-EGFP mice were shipped to UVM and the offsprings were used for these studies. All PACAP-EGFP mice were genotyped by PCR for EGFP expression (forward: 5'-TCTTTGCTCAGGGCGGACTG -3'; reverse: 5'- GCACCATCTTCTTCAAGGACGAC -3'). All animals were housed under a 12-hour light/dark cycle (lights on 0700 h) with food and water available ad libitum, and habituated to the animal facility for at least one week prior to any experiments. All procedures were approved by the Institutional Animal Care and Use Committee at the University of Vermont.

**Neuropathic Pain Model**

Chronic constriction injury (CCI) of the sciatic nerve was performed in rats as described previously (2). Rats were anesthetized with 2 - 3% isoflurane and four loose ties (4-0 chromic gut sutures, Ethicon) were placed unilaterally midthigh proximal to the trifurcation of the sciatic nerve. In sham surgeries, the sciatic nerve was briefly exposed and the muscles repositioned before incision closing with wound clips. In some experiments with intra-amygdalar infusions, the stereotactic surgery for cannula implantation was performed concurrently with CCI (see below). In PACAP-EGFP mice, the same CCI procedure was followed except only three chromic gut sutures were used. Animals were allowed 7 - 10 days post surgical recovery before any testing. During this period, all animals were monitored, handled and weighed daily.

**Intra-Amygdalar Infusion**

Rats were prepared for intra-amygdalar infusions using procedures described previously (3, 4). The rats were anesthetized with isoflurane vapor and secured in a stereotaxic apparatus. After skin incision, the skull was exposed and four screws were inserted to provide skullcap stability. Two stainless steel guide cannulae (22GA, PlasticsOne, Roanoke, VA) were placed for bilateral targeting of the CeA using coordinates (from bregma in mm) AP: -2.6, ML: ± 4.5, DV: -7.2 from the surface of the dura; a dummy cannula was inserted to ensure guide cannula patency. A skullcap was created with dental cement to hold the cannula in place. For acute antagonist, drug or vehicle administration, the rats were lightly restrained with a cloth towel and the dummy cannula was replaced with an internal cannula, extended 1mm distally, for automated infusions at 0.5 µl/min (Harvard Apparatus, Holliston, MA). Following infusion, the internal cannulae were left in place for 1 min to allow drug dispersion before removal. Infused compounds included PACAP38 (1 µg/0.5 µl), PACAP(6-38) (0.3 µg/0.5 µl), Pitstop 2 (30 µM/0.5 µl) and PD98059 (20 µM/0.5 µl). Infusion for each compound was 0.5 µl; vehicle contained 0.05% BSA

in saline. The animals were returned to their home cages for 30 min before testing (see timeline Figure 3A).

**Histological and Immunocytochemical Procedures**

The PACAP-EGFP mice were deeply anesthesized with isoflurane and perfused transcardially first with phosphate buffered saline, followed by 4% paraformaldehyde before tissue dissection. The brains were removed following cranium removal along the suture lines. The vertebral column was exposed and the laminae plates transected with iris scissors along the length of the column to remove the spinous processes. The spinal cord was removed en bloc; the sciatic nerve and L3 - L5 dorsal root ganglia were identified and also removed. The tissues were postfixed overnight in 4% paraformaldehyde, rinsed in phosphate buffer, and equilibrated in a graded sucrose series (to 30% sucrose final) before embedding in OCT compound (ThermoFisher Scientfic, Waltham, MA) and freezing in a dry ice/alcohol slurry. Cryosections (30 µm) were prepared and mounted onto subbed slides for inspection of endogenous EGFP signals on a fluorescence microscope (below).

For immunocytochemistry and histological staining, the animals were anesthesized and prepared 1 h following drug infusions and/or behavioral testing. The animals were perfused transcardially as above with 4% paraformaldehyde and the brains were postfixed for 24 h, washed and equilibrated in 30% sucrose before embedding in OCT compound for cryosectioning (30 µm). The sections were mounted onto subbed slides, permeabilized with 0.3% Triton X-100 and blocked with 1% BSA. For immunocytochemical processing, the tissue sections were encircled using a PAP pen to create a hydrophobic barrier before application of primary antibody. Immunocytochemical staining for PACAP (1:10, 48 h at 4°C, Jens Hannibal, Bisperg Hospital, Copenhagen, Denmark) was enhanced by tyramide signal amplification (Perkin Elmer, Waltham, MA) for visualization with streptavidin-conjugated cyanine (Cy2 or Cy3)

compounds, as previously described (5). The antibody is directed to the N-terminus of PACAP and hence does not discriminate between PACAP27 and PACAP38; importantly, the antibody does not recognize VIP. From high antibody specificity and low background signal, the PACAP localizations were performed using tyramide amplification as previously described (5). After primary antibody incubation and washings, the cryosections were incubated in biotinylated horse secondary antibody (1:200; Vector Laboratories, Burlingame, CA) for 2 hours. The sections were then washed, treated with streptavidin horseradish peroxidase (HRP; 1:250) for 30 min, washed again and subsequently incubated in a tyramide-biotin reagent (1:100; Perkin Elmer, Boston, MA) for 10 min. After extensive buffer rinses, the PACAP immunoreactivity in the sections was localized using 1:200 avidin-conjugated Cy2 or Cy3 (Jackson ImmunoResearch, West Grove, PA) for 2 h. Detection for phosphorylated ERK (pERK; 1:1000, #4370; Cell Signaling Technology, Danvers, MA), β-arrestin1 and 2 (1:1000; #4674; Cell Signaling Technology, Danvers, MA), c-Fos (1:300, sc-52 Santa Cruz Biotechnology, Dallas, TX), vGlut1 (1:1000, AB5905; Millipore Billerica, MA), vGlut2 (1:1000, AB2251; Millipore Billerica, MA) and GAD (1:300, AB1511; Millipore Billerica, MA) were performed similarly using species-specific AlexaFluor 488 or Cy3-conjugated secondary antibodies (1:250, 2 h; Jackson ImmunoResearch, West Grove, PA). For antigen exposure, the sections for pERK immunoreactivity were treated with 10% methanol for 15 min prior to the blocking step. Some sections were also processed using the avidin-biotin complex (ABC) immunocytochemical methods (Vector Laboratories, Burlingame, CA) for visualization with diaminobenzidine (DAB). For these procedures, the sections were permeabilized, treated with 3% hydrogen peroxide in methanol (10 min) to exhaust endogenous peroxidase activity and incubated in blocking solution. Following primary antibody incubation, the sections with incubated with 1:200 biotinylated secondary antibody (2 h) followed by 1:400 of the ABC complex (2 h). The sections were washed extensively and incubated for 15 min in substrate solution containing 0.3 mg/ml diaminobenzidine and 0.075% hydrogen peroxide in 50 mM Tris buffer, pH 7.4. The specificity

of the PACAP antibody has been well characterized (5), including from work in our laboratory (4). The pERK antibody detects only phosphorylated p42/p44 protein bands on Western blots and has been used in immunocytochemical studies in our laboratory (6, 7); similarly, the β-arrestin antibody uniquely identifies arrestin proteins in our Western assays. The specificity and application of the c-Fos, vGlut and GAD antibodies has been described in previous studies (8-11). For light counterstaining and cannulae placement verifications, the tissue sections were incubated treated with 0.1% cresyl violet stain and processed using standard histological procedures.

**Image Analysis**

Micrographs were acquired with a 20x objective using a Nikon (Melville, NY) C1 confocal scanner attached to a Nikon Eclipse E800 microscope (Micro Video Instruments, Avon, MA) and Olympus fluorescence microscopes using EZ-C1 v3.4 (Nikon Instruments, Melville, NY) and StereoInvestigator (MBF Biosciences, Williston, VT) software, respectively. The corresponding CeA fields in the different brains were identified using the hippocampus and optic tracts as reference points and landmarks. All images for each study were acquired under identical settings and parameters, and the image data files were exported to NIH ImageJ (12) for quantitative image analyses to threshold, determine signal area (pixel number in staining area) and calculate correlation coefficients (3, 4). For fiber/puncta EGFP or peptide immunoreactivity, the number of thresholded pixels per unit area was quantitated. For enumeration of pERK, c-Fos, and PACAP-EGFP$^{+}$ cells in prescribed areas, a semi-autonomous cell counting method was performed in ImageJ. All data represent mean values ± SEM.

## Behavioral Assessments

### *Open Field*

Open field behavioral testing was performed after the thermal baseline measurements were completed (Figure 2A, timeline). Thirty min following CeA infusions, the rats were individually placed into the corner of a 75 cm x 75 cm opaque black open arena with 50 cm walls (United States Plastics Corp., Lima, OH) illuminated at 20 lux using a red bulb. Rat arena center entries (18 cm x 18 cm square) and total distance traveled over 5 min test sessions were digitally captured using a ceiling mounted camera for analyses using EthoVision XT version 6.1.326 (Noldus Information Technology, The Netherlands) as described previously (4). Each rat was exposed to the test once to avoid repeated open field stressor responses; 30 minutes after the open field tests the animals were assessed for thermal sensitivity. Rats were always exposed to open field test first to avoid any confounding thermal sensitivity stress effects.

### *Thermal Sensitivity Assessment*

Approximately 7 - 10 days after surgery, the rats were habituated in the Hargreave's thermal apparatus chamber (Plantar Analgesia Meter, IITC Life Science Inc., Woodland Hills, CA) in 4 daily sessions (30-min session per day for 4 days; no thermal testing). The elevated clear acrylic testing chamber was atop a glass floor containing internal heating element that heated the glass to a consistent 30°C. Following habituation, the animals were given 3 baseline thermal tests on each hindpaw (legs with ipsilateral ligated and contralateral non-ligated nerves) to assess thermal latency times. Responses to thermal stimuli were tested using a low intensity guide light (8% active intensity) to target the hindpaw and a beam of focused radiant light (4 X 6 mm, set to 25% of active intensity) from the apparatus beneath the glass floor was delivered to the plantar surface of the paw. Upon withdrawal or licking of the hindpaw, the heat source was immediately terminated and the reaction time automatically recorded. An automatic cut-off timer

set at 30 sec was built into the system to prevent tissue damage. The hindpaws were randomly selected at trial initiation and 3 trials separated by 5 min inter-trial intervals were performed on each of the left and right hindpaws. Only animals that developed baseline thermal hypersensitivity in the sciatic nerve-ligated leg, established as greater than a 10% decrease in thermal latency time compared to the contralateral (unoperated) leg in Hargreave's assay were used for testing and analyses. Approximately 90% of the CCI animals developed thermal hypersensitivity and passed criteria for testing.

**Transcript Analysis**

Quantitative PCR (QPCR) was performed in the same manner as previously described (4, 13, 14). Following brief isoflurane anesthesia and rapid decapitation, rat brains were quickly frozen in OCT compound (ThermoFisher Scientfic, Waltham, MA); 300 µm cryosections were prepared and 740 µm micropunches from each region were harvested. Total RNA extraction was performed using STAT-60 RNA/mRNA isolation reagent (Tel-Test "B", Friendswood, TX). Each set of brain regions was reverse transcribed simultaneously using random hexamer primers using SuperScript II Preamplification System (Invitrogen, Carlsbad, CA). The cDNA templates were diluted 10-fold and assayed on an ABI Prism 7500 Fast Real-Time PCR System (Applied Biosystems, Foster City, CA) using SYBR Green I JumpStart Taq ReadyMix (Sigma, St. Louis, MO) containing 5.0 mM MgCl2, 200 µM dATP, dGTP, dCTP and dTTP, 0.64 U Taq DNA polymerase and 300 nM of each primer in a 25 µl reaction volume. Oligonucleotide primers were as follows: PACAP (S) 5'-CATGTGTAGCGGAGCAAGGTT-3' (AS) 5'-GTCTTGCAGCGGGTTTCC-3', PAC1 (S) 5' -AACGACCTGATGGGACTAAAC-3' (AS) 5'-CGGAAGCGGCACAAGATGACC-3'. Following amplification, melting profiles of amplicons were used to verify unique product generation. A standard curve constructed in the same QPCR run by amplification of serially 10-fold diluted plasmids containing the target sequence was used for

analysis. Increase in SYBR Green I fluorescence intensity (ΔRn) was plotted as a function of cycle number and threshold cycle (CT) was determined using software as the amplification cycle at which the ΔRn intersects the established baseline. Transcript levels were calculated from the CT by interpolation from the standard curve. For each target sequence, all samples from the same brain region were amplified simultaneously. All data was normalized to 18s RNA and calculated as a fold change from control.

The PAC1 receptor primers are directed at the N-terminal extracellular domain of the receptor and hence recognize all PAC1 receptor variants. The major receptor variants depend on the alternative splicing of two 84 bp Hip and Hop cassettes that generate inserts into the third intracellular loop (13), a region important for G protein binding and selectivity. Consequently, the variants of PAC1 may be null (containing neither Hip nor Hop), Hip, Hop, and Hop2 variant or Hiphop. All rodent brain regions express the null and Hop PAC1 receptor isoform with the null being the more prevalent form. Despite one report to the contrary (15), our ongoing studies suggest that chronic stress and pain do not appear to alter significantly PAC1 receptor alternative splicing and null:Hop receptor transcript expression ratio (May and Braas, unpublished observations).

**Cell Culture**

A stable HEK PAC1-EGFP receptor cell line was used for PAC1 receptor internalization studies. The preparation of the cell line was described in detail previously (6, 7). In brief, HEK 293 cells were transfected with a human PAC1 receptor construct tethered at the carboxyl-terminus to an EGFP-encoding cassette. The cells were cultured in Dulbecco's modified Eagle's medium/F-12 containing 8% fetal bovine serum and 500 μg/ml Geneticin for stable cell selection by limiting dilutions. Functional expression of the receptor was assessed by endogenous EGFP fluorescence and PACAP-stimulated second messenger activation. Under unstimulated basal conditions, the PAC1-EGFP receptor fluorescence is localized primarily on the cell surface. For

PAC1 receptor internalization studies, the cells were cultured on glass coverslips and at 70% confluence treated with 25 nM PACAP27 peptide (final concentration) for 15 min before fixation in 4% paraformaldehyde for 15 min and fluorescence microscope inspection. In antagonist studies, the cultures were pretreated with 1 µM PACAP(6-38) for 15 min before subsequent addition of 25 nM PACAP27 for 15 min. For pERK and arrestin immunocytochemistry, the cultures were treated and fixed cells were permeabilized, treated with 10% methanol for 10 min (for pERK only), blocked and processed exactly as described above using Cy3-conjugated secondary antibody.

**Western Blot**

Control and treated HEK PAC1-EGRP receptor cultures were extracted as previously described (6, 7) with 75 µl RIPA buffer (50 mM Tris-HCl, pH 8.0, 120 mM NaCl, 5 mM EDTA, 1% NP-40, 0.1% SDS) containing 0.3 mg/ml phenylmethylsulfonylfluoride, protease inhibitors (16 µg/ml benzamidine, 2 µg/ml leupeptin, 50 µg/ml lima bean trypsin inhibitor, 2 µg/ml pepstatin A) and phosphatase inhibitor mix (5 mM EDTA, 5 mM EGTA, 1 mM sodium orthovanadate, 10 mM sodium pyrophosphate, 50 mM sodium fluoride) (6, 7). Total sample proteins were determined using the BCA reagent (Pierce Biotechnology, Rockford, IL). For Western analyses, protein samples (30 µg) were fractionated on 4 - 12% SDS-PAGE gels, transferred onto Immobilon-P PVDF membranes (Millipore, Billerica, MA), blocked and incubated with primary antisera to pan and pERK1/2 (1:5000; Cell Signaling Technology, Beverly, MA) for quantitative infrared imaging (LiCor Biosciences, Lincoln, NE).

**Statistics**

All statistical tests were performed in SPSS (version 22) and GraphPad PRISM (version 6). Two-way analysis of variance (ANOVA) was performed to examine main effects and

interactions, and Bonferroni's multiple comparisons tests were used to compare different groups for all experiments except where noted. A multifactorial ANOVA was used to examine PACAP(6-38) treatment with CCI condition across side and day in thermal sensitivity tests. Student's t-tests were performed to compare changes in average weight gain and post-surgery weight loss.

**Experimental Procedures**

*Experiment 1 - PACAP/PAC1 receptor transcript analyses after CCI*

Adult male rats received sham or CCI procedures (n = 8 per group) and after post surgical recovery, placed in a Hargreave's apparatus for thermal sensitivity testing (day 13 following surgery). The next day the animals were anesthetized and euthanized by decapitation. The brains were immediately removed (no fixation), blocked and frozen in cryoprotectant. From cryosections (300 µm), select brain regions were micropunched (740 µm) for transcript analyses as described in Methods.

*Experiment 2 - CCI-induced CNS/PNS PACAP expression in PACAP-EGFP transgenic mice*

PACAP-EGFP mice with sham (n = 8) or sciatic nerve chronic constriction injury (CCI, n = 8) were allowed 14 days post-surgical recovery before deep isoflurance anesthesia and transcardial 4% paraformaldehyde perfusion as described in Methods. The L3 - L5 dorsal root ganglia (DRG), corresponding spinal cord segments, sciatic nerves and brains were removed and blocked in Tissue Tek OCT compound; cryosections from the ipsilateral (injury/sham) or contralateral (non-operated) tissue structures were mounted onto subbed slides for additional processing for inspection for endogenous EGFP fluorescence as described in figure legends (Fig 1 and Fig 2).

*Experiment 3 - Attenuation of CCI responses with PAC1 receptor antagonist PACAP(6-38)*

The time line for these studies is shown in Figure 3A. Adult male rats received sham or CCI procedures, and CeA cannula implants in the same surgical session, as described in Methods. The rats were randomly divided into 4 groups (sham-vehicle; sham-PACAP(6-38); CCI-vehicle and CCI-PACAP(6-38); n = 8 per group) and handled daily for weight measurements. There was no difference in the pre-surgery weights of rats in these studies (Sham, 362 ± 16 gm vs CCI, 369 ± 14 gm). Following 7 - 10 day post-surgical recovery, the animals were habituated in the Hargreave's thermal testing chamber for 30 min each day for a total of 4 days. On the following day, the animals were assessed for baseline thermal sensitivity in both hindpaws in a series of trials (3 trials for each hindpaw) as described in Methods and rats that demonstrated CCI-induced nociceptive hypersensitivity were used for testing the next day (see Methods for criteria). The animals received bilateral CeA infusions with vehicle or drug and after 30 min, placed in the open field test for 5 min; the open field test was always administered first. The animals were then returned to their home cages and after 30 min, evaluated on the Hargreave's thermal apparatus for nociceptive responses (3 trials with 5 min intervals between trials for each hindpaw selected at random). An hour after the last test, the animals were euthanized and the fixed tissues collected, processed and cryosectioned for immunocytochemistry and cannula placement verification. The order of the animals tested was random and observer/handler in the tests was blinded with respect to drug treatments.

*Experiment 4 - Localization of CCI-induced ERK activation with PACAP and neurotransmitter markers*

Adult male rats received sham or CCI surgical procedures (n = 8 per group) and after post surgical recovery and Hargreave's thermal sensitivity testing (14 days total), the animals were anesthetized and perfused transcardially with 4% paraformaldehyde for tissue collection. The

brain cryosections were mounted onto subbed slides and dually immunocytochemically processed for PACAP and pERK, VGlut1, VGlut2 or GAD immunoreactivity as described in Methods. The personnel performing the imaging and analyses were blinded to the different animal groups.

*Experiment 5 - Attenuation of CeA PACAP-induced nociceptive and pERK responses with inhibitors to ERK activation and endocytosis*

Adult male rats received bilateral cannula implants into the CeA as described in Methods and were divided randomly into 6 groups (n = 7 - 8 per group). After post-surgical recovery and baseline Hargreave's thermal assay testing (4 days habituation and 1 day of baseline testing, as above), the rats were infused with vehicle, PACAP38, drug alone (PD98059 or Pitstop 2), or drug + PACAP38. In drug + PACAP38 infusions, the drug was administered first followed by PACAP38 injections 30 min after the pretreatment. Thirty minutes after PACAP injection, the animals were tested on the Hargreave's thermal apparatus; 1 hour following PACAP injection the animals were anesthetized and euthanized by transcardial fixative perfusion for tissue processing. The mounted cryosections were immunocytochemically processed for PACAP, pERK and c-Fos immunoreactivity.

*Experiment 6 - Attenuation of PACAP-stimulated ERK activation and receptor internalization with PACAP(6-38) in PAC1-EGFP receptor cells*

Culture HEK cells stably expressing PAC1-EGFP receptor were cultured in 24 well tissue culture plates and treated with vehicle or 25 nM PACAP; replicate wells were pretreated with 1 μM PACAP(6-38) for 15 min before 25 nM PACAP addition. After 15 min PACAP exposure (maximal pERK induction from previous time course experiments), the cultures were harvested with RIPA lysis buffer containing protease and phosphatase inhibitors. The cell extracts were fractionated by gel electrophoresis for quantitative Western analyses for pERK induction as

described in Methods. The immunoblots were stripped and the reprobed with antisera for pan ERK for total ERK estimation in all samples.

PAC1-EGFP receptor cells were also cultured on 10 mm glass coverslips and treated with 25 nM PACAP, in the absence or presence of PACAP(6-38) exactly as above. After 15 min PACAP treatment, the cultures were fixed and immunocytochemically processed for pERK immunoreactivity using a Cy3-secondary antibody conjugate to allow dual PAC1-EGFP receptor (green) and activated ERK (red) imaging on a fluorescence microscope.

*Experiment 7 - PACAP-stimulated PAC1-EGFP receptor trafficking to endosomes*

PAC1-EGFP receptor cells cultured on glass coverslips were similarly treated with PACAP and fixed for immunocytochemical processing for β-arrestin immunoreactivity using a Cy3-secondary antibody conjugate. Colocalization of PAC1-EGFP receptor and β-arrestin immunoreactivity allowed receptor tracking into endosomes.

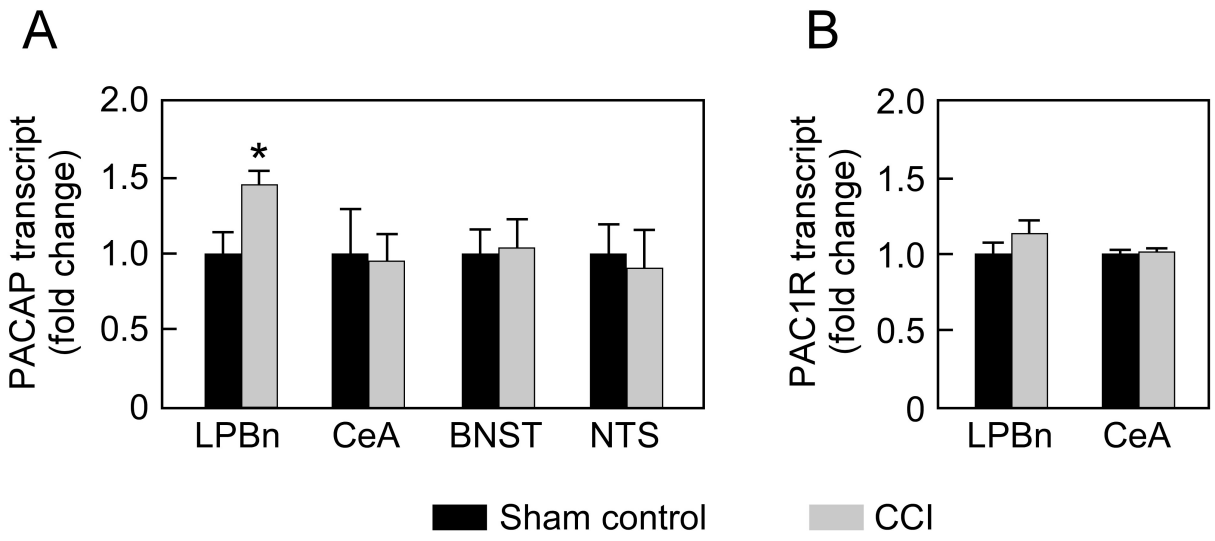


**Figure S1.** CCI increases LPBn PACAP transcripts. Adult male rats underwent either CCI or sham surgery and after 14 days, the indicated brain regions were harvested for quantitative PCR analyses. CCI increased LPBn PACAP transcript levels compared to sham tissues (CCI 1.47 ± 0.1 vs sham 1.00 ± 0.2, $t(12) = 2.36$, *$p = 0.036$). CCI had no effects on PACAP transcripts in the CeA (CCI 0.96 ± 0.2 vs sham 1.00 ± 0.3, $t(12) = 0.12$, $p = 0.9$), anterolateral BNST (CCI 1.06 ± 0.2 vs sham 1.00 ± 0.2, $t(13) = 0.21$, $p = 0.8$), or the solitary nucleus (NTS) (CCI 1.00 ± 0.2 vs sham 0.90 ± 0.3, $t(14) = 0.29$, $p = 0.8$). There were no effects of CCI on PAC1 receptor transcript levels in the tissues examined: LPBn (CCI 1.15 ± 0.1 vs sham 1.00 ± 0.1, $t(12) = 1.09$, $p = 0.3$); CeA (CCI 1.03 ± 0.1 vs sham 1.00 ± 0.1, $t(12) = 0.45$, $p = 0.7$). n = 6 - 8 per group; data represent mean fold change normalized to 18S ± SEM.

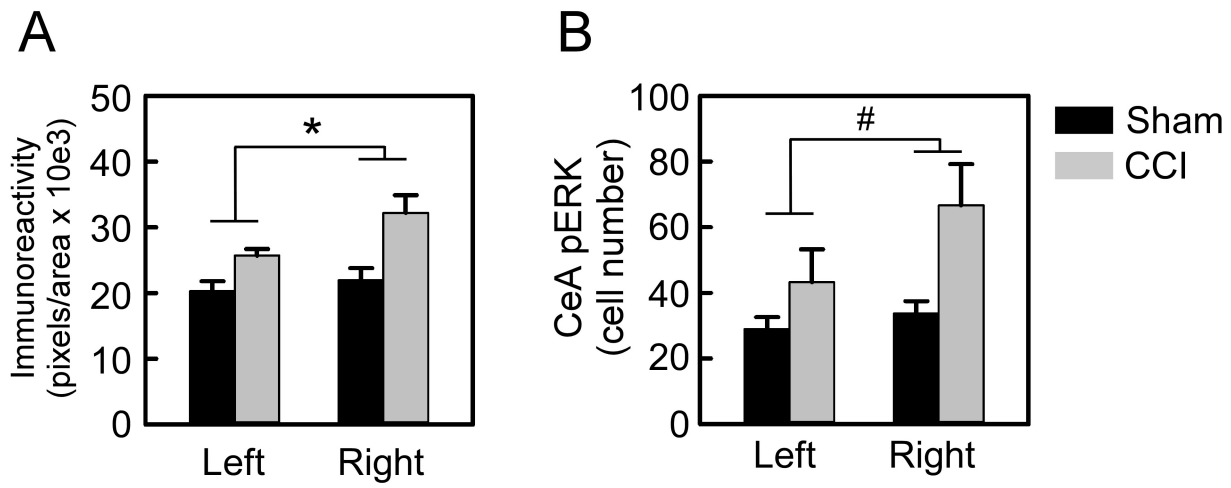


**Figure S2.** The CeA demonstrates lateralization in CCI-induced increases in PACAP and pERK immunoreactivity. CCI (14 days) preferentially increased PACAP immunoreactivity and $pERK^+$ cells in the right CeA. When thresholded PACAP immunoreactivity from Figure 1 was analyzed with respect to right or left CeA, there was a significant main effect of side (A; $F(1,28) = 7.61$, *p = 0.01), but no interaction ($F(1,28) = 4.87$, p = 0.4), with greater PACAP immunoreactivity in the right CeA. There was a similar bias in $pERK^+$ cells in the right CeA with a trend for the effect of side (B; $F(1,26) = 3.15$, #p = 0.09). These results appear consistent with the lateralization of CeA pERK shown previously in persistent pain, and implicate PACAP in the lateralization of the nociceptive process. As in Figure 1, n = 6 - 7 per group, 3 sections enumerated per side per animal.

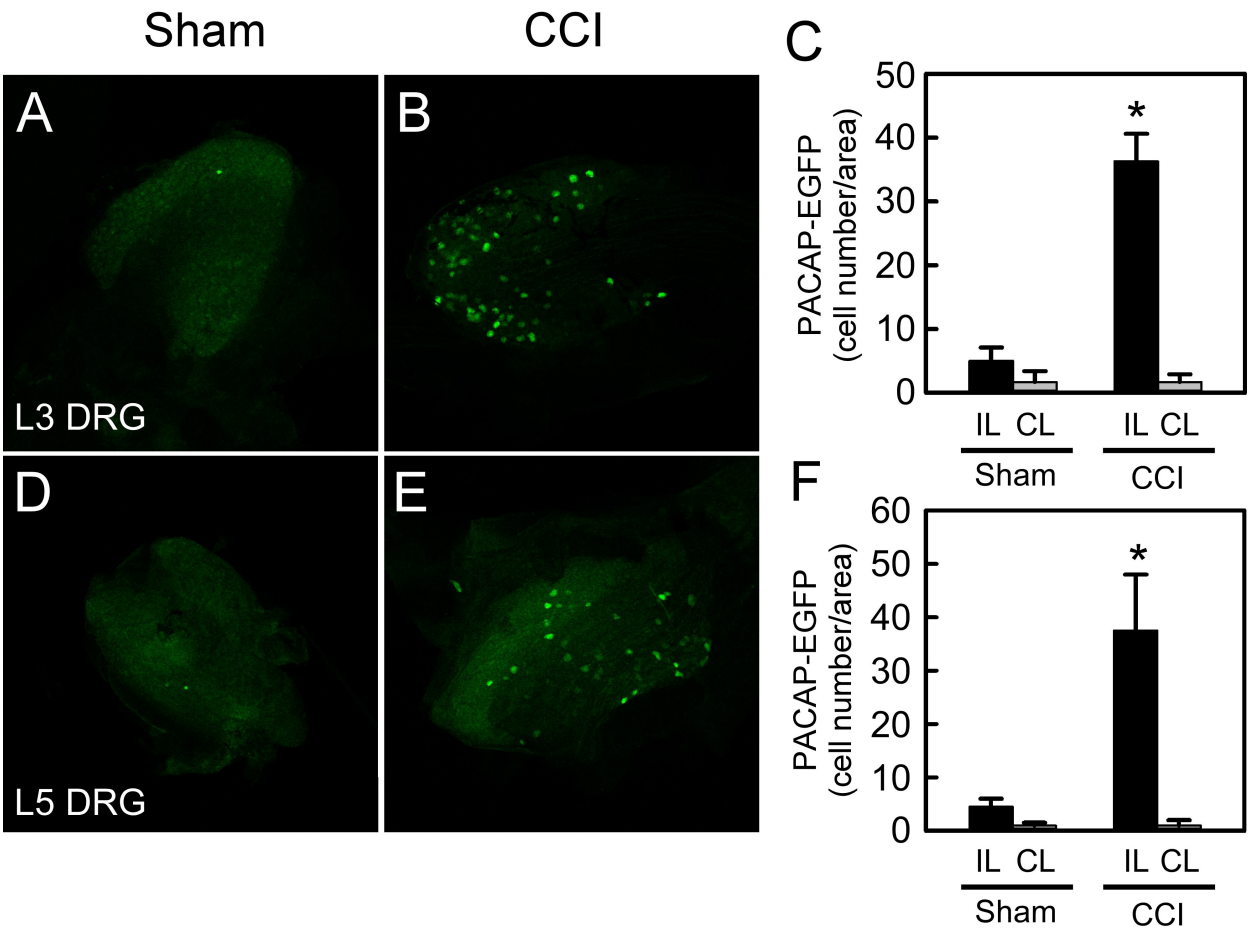


**Figure S3.** CCI increases PACAP-EGFP expressing L3 and L5 DRG neurons. Similar to the L4 DRG (Figure 2), unilateral CCI increased the number of L3 and L5 DRG PACAP-EGFP$^{+}$ neurons 14 days postsurgery (B, E) compared to sham controls (A, D). L3 - L5 DRG peripheral sensory axons travel in the sciatic nerve with major contributions from L4. Accordingly, the fold increase in CCI-induced PACAP-EGFP+ neuron expression in L3 DRG (C; sham ipsilateral = 5.0 ± 2.1 cells vs CCI ipsilateral = 36.3 " 4.3 cells, *p = 0.0002, n = 3 per group) and L5 DRG (F; sham ipsilateral = 4.5 ± 1.5 cells vs CCI ipsilateral = 37.5 ± 10.5 cells, *p = 0.0002, n = 3 per group) was not as robust as that in L4 DRG. Data represent mean cells/unit area ± SEM.

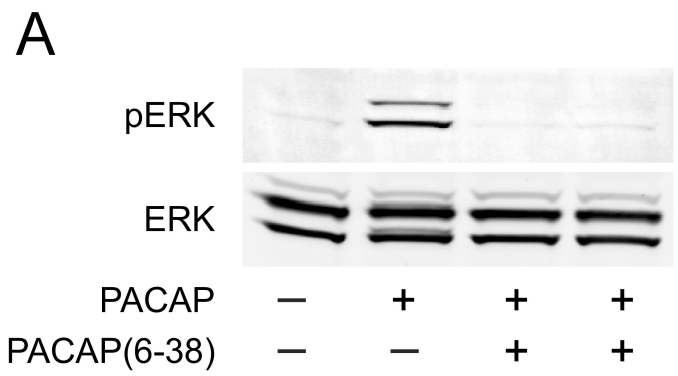


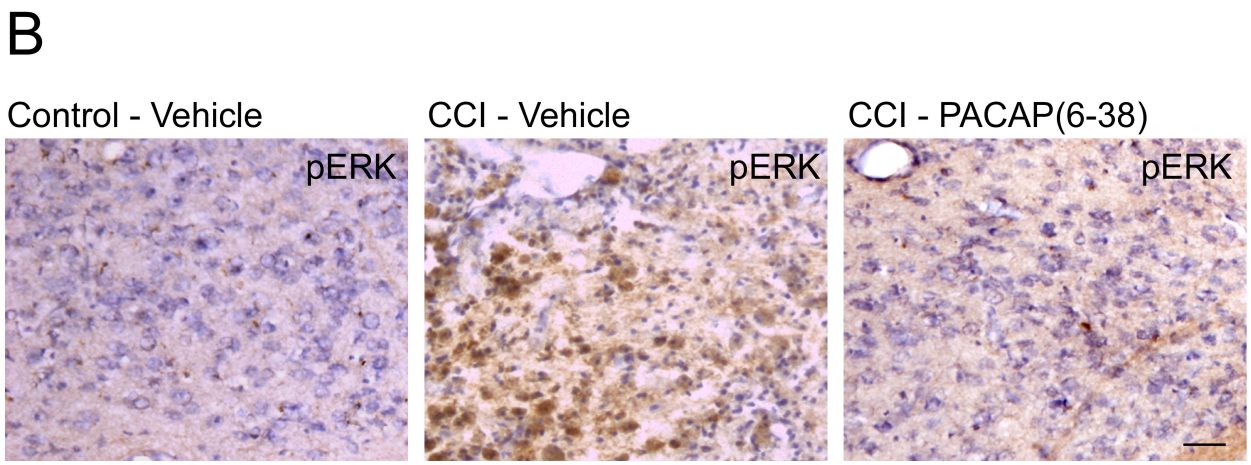


**Figure S4.** PACAP(6-38) blocks PACAP and CCI-stimulated ERK activation. A, HEK PAC1-EGFP receptor cells were pretreated with vehicle or 1 µM PACAP(6-38) for 15 min at 37°C before subsequent 10 min exposure to 25 nM PACAP27. The cells were immediately lysed in RIPA buffer containing protease and phosphatase inhibitors as described in Methods. Following SDS-PAGE fractionation, the protein bands were transferred to membranes for Western analysis using pERK specific antibodies (top panel). The blots were subsequently stripped and reprobed with a pan-ERK antibody to demonstrate comparable sample loading among wells. PACAP(6-38) was able to completely block PACAP-induced cell ERK activation. pERK and ERK proteins appear as dual p44/p42 (44 and 42 kDal) bands. B, The CeA of control and CCI rats were infused with vehicle or PACAP(6-38) as described in Methods and processed for pERK immunoreactivity using the avidin-biotin complex technique to allow tissue visualization. Following substrate development with DAB/H202 (brown reaction products), the sections were counterstained with cresyl violet. As in Western analyses, PACAP(6-38) was able to block CCI-induced ERK activation. Representative data from n = 3 animals per group. Scale bar = 50 µm.

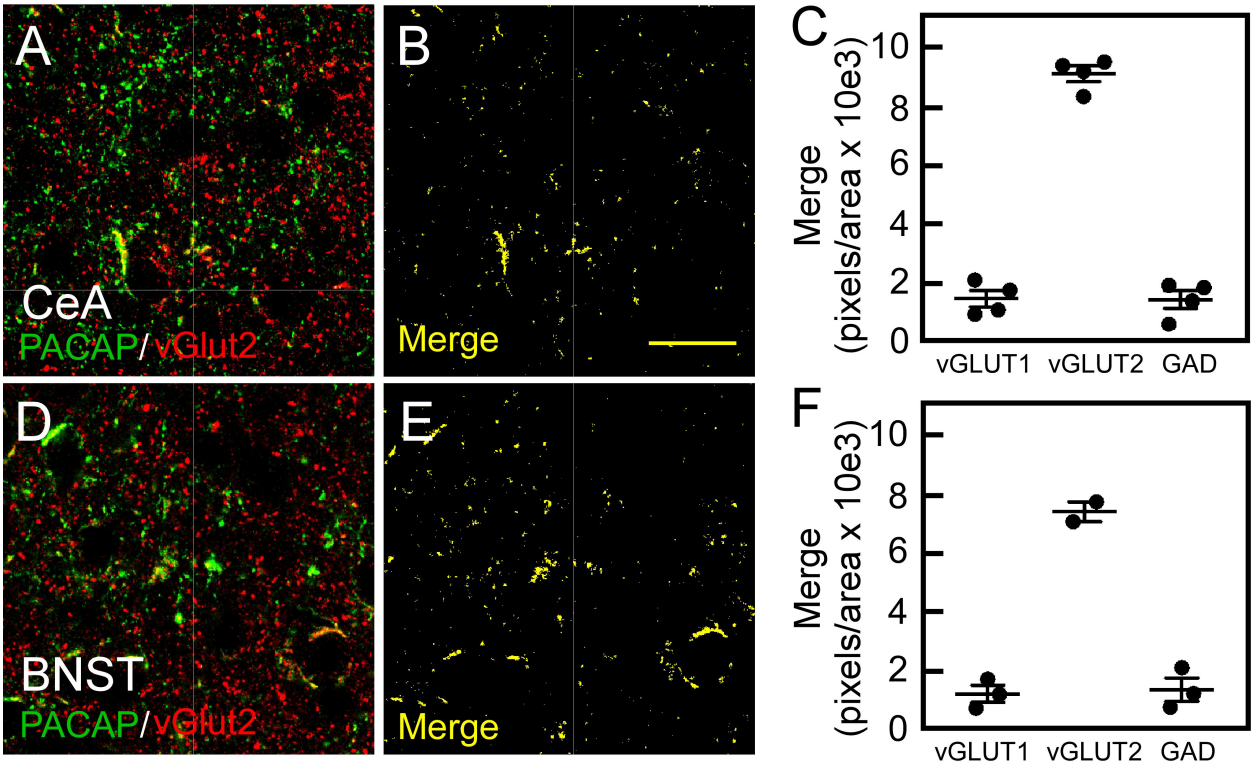


**Figure S5.** CeA and BNST PACAP fibers colocalize predominantly with vGlut2 immunoreactivity. CeA (A) and BNST (D) tissues were dually processed for PACAP (Alexa Fluor 488, green) and vGlut2 (Cy3, red) to help establish neuronal transmitter identity. CeA and BNST PACAP colocalized with glutaminergic marker vGlut2 as shown in their respective isolated merged signals (B, E; yellow). From quantitative image analyses, there was minimal overlap between PACAP and vGlut1 or GAD (C, F; see Figure S5). n = 7 - 8 animals per group. Scale bar = 25 µm.

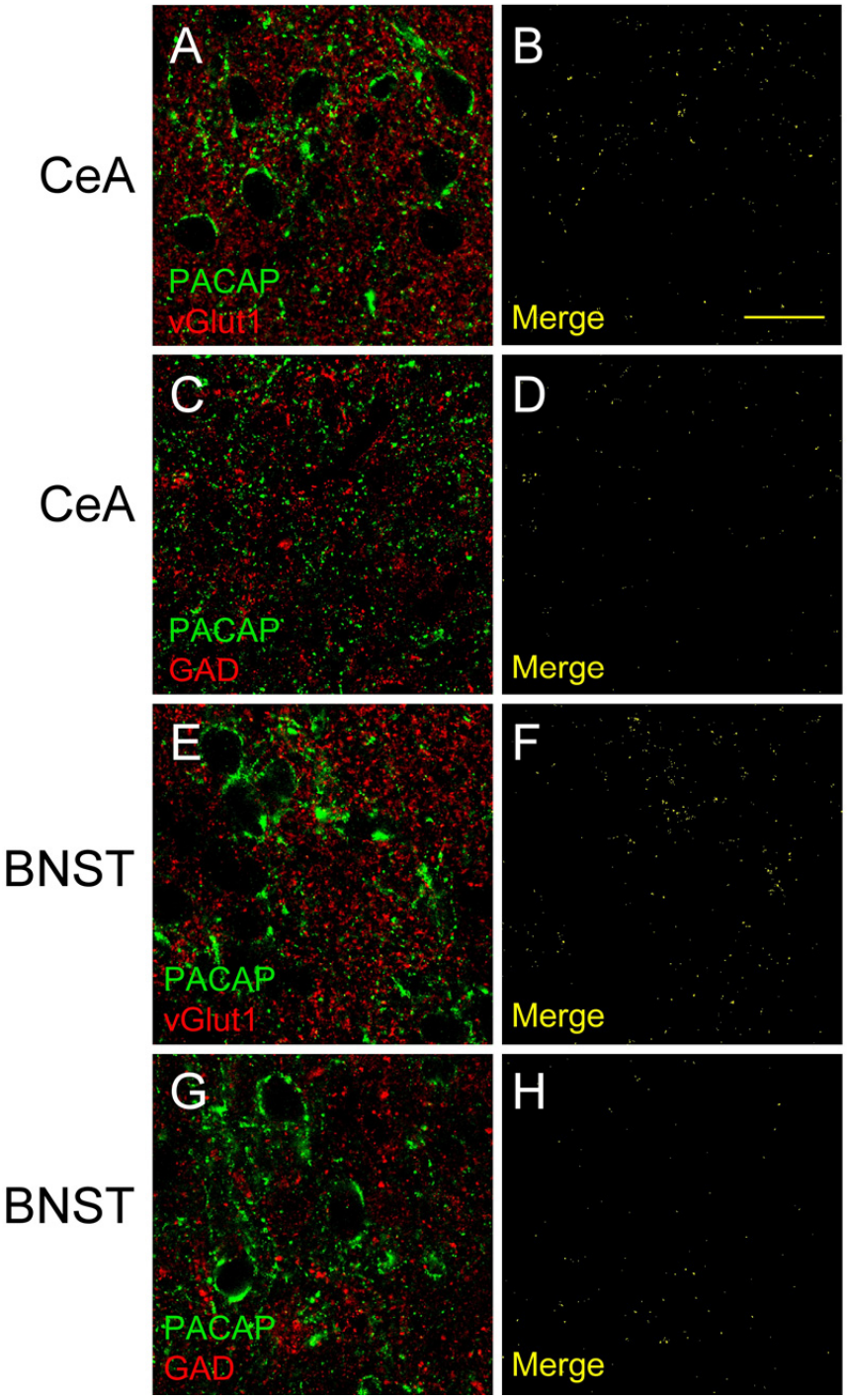


**Figure S6.** CeA and BNST PACAP immunoreactivity does not colocalize with vGlut1 or GAD. CeA (A, C) and BNST (E, G) tissues were dually processed for PACAP (Alexa Fluor 488, green) and vGlut1 (Cy3, red) or GAD (Cy3, red). Unlike vGlut2 (Figure S4), there was little overlap with the glutamatergic marker vGlut1 or GABAergic marker GAD in both regions as shown by the paucity of merged signals (B, D, F and H; yellow). Quantitative analyses in Figure S4. n = 7- 8 animals per group. Scale bar = 25 µm.

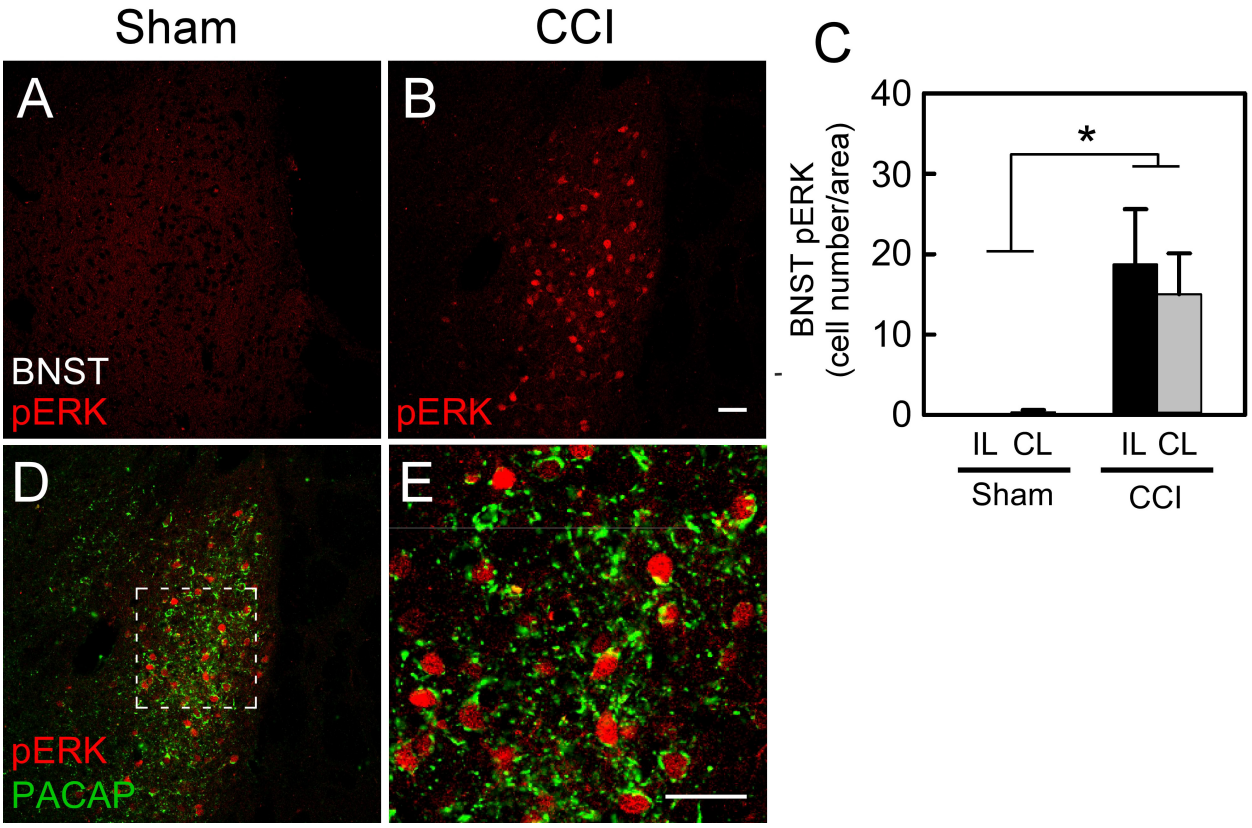


**Figure S7.** PACAPergic fibers contact BNST pERK+ neurons in CCI. As in the CeLC, CCI increased bilaterally the number of pERK+ neurons in the anterolateral BNST compared to sham controls (A - C). The BNST pERK+ cells (Cy3, red) were in close contact with PACAP fibers (D,E; Alexa Fluor 488, green), implicating PACAP as a potential mechanism of CCI-induced nociceptive ERK signaling. There is a main effect of CCI (C; $F(1,8) = 15.3$, *$p = 0.005$, $n = 3$ animals per group). Scale bar = 50 µm.

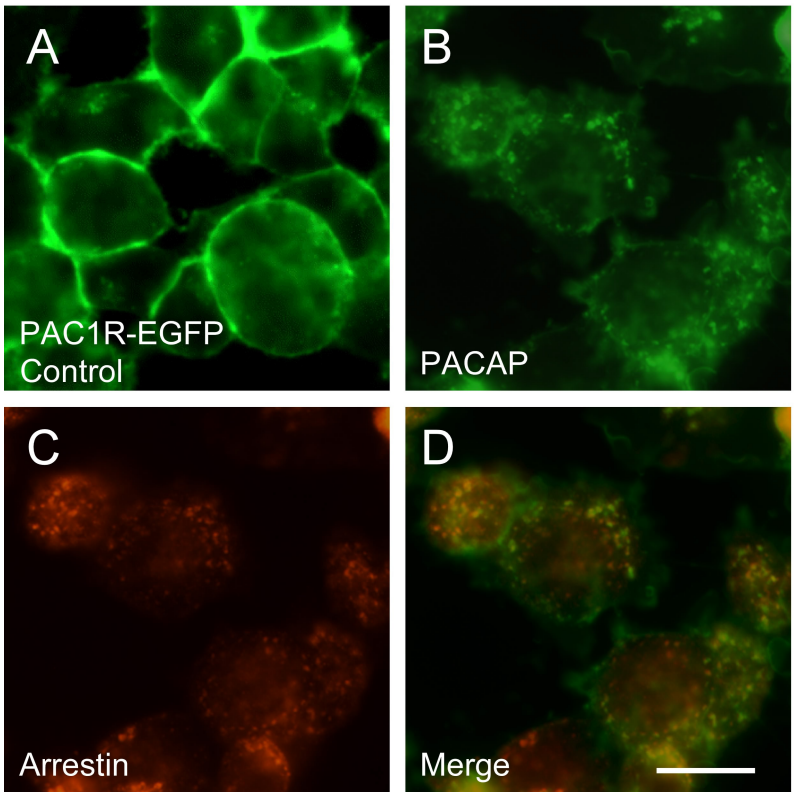


**Figure S8.** Internalized PAC1 receptors can be colocalized with β-arrestin in endosomes. In control unstimulated conditions, PAC1-EGFP receptor fluorescence was localized to the plasma membrane that appeared to circumscribe the HEK cells (A). The application of 25 nM PACAP27 to the cultures rapidly induced PAC1 receptor internalization into vesicular endosomal structures with a concomitant depletion of PAC1-EGFP fluorescence on the cell surface (B). β-arrestin GPCR binding and recruitment to endosomes for MEK/ERK scaffolding and signaling have been well established (16, 17). When the PACAP stimulated PAC1-EGFP receptor cells were fixed and immunocytochemically process for β-arrestin immunoreactivity for visualization with a Cy3-secondary antibody conjugate, a large fraction of the internalized PAC1-EGFP receptors into vesicles (green, B) was colocalized with β-arrestin immunoreactivity (red, C; merged vesicles in yellow, D). These data illustrate that internalized PAC1 receptors can be trafficked to endosomes for sustained ERK signaling. Representative data from 3 separate culture wells. Scale bar = 10 µm.

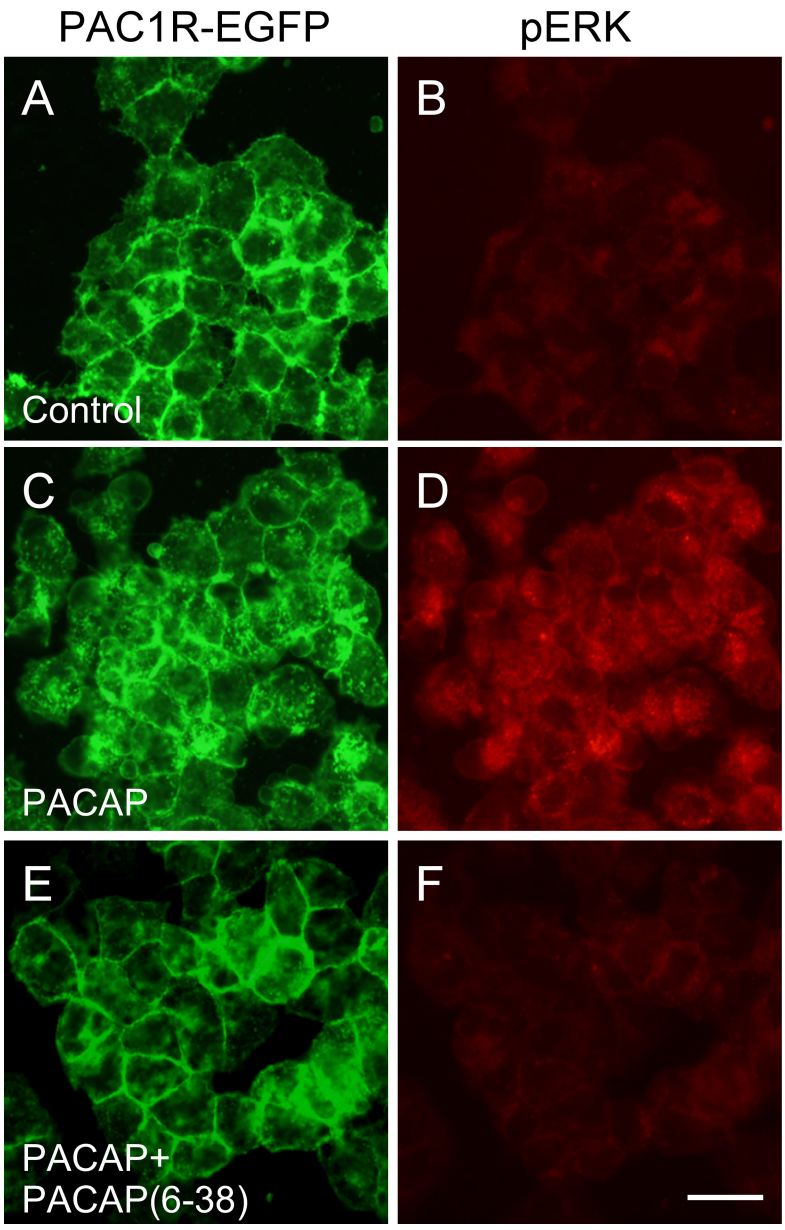


**Figure S9.** PACAP(6-38) blocks PACAP-stimulated PAC1-EGFP receptor internalization and ERK signaling. Untreated control HEK PAC1-EGFP receptor cells demonstrate receptor expression on the cell surface (A) and low basal levels of ERK activation (B). Culture treatment with 25 nM PACAP27 for 10 min resulted in PAC1-EGFP receptor internalization in parallel with increased cellular pERK immunoreactivity (panels C and D). However, culture pretreatment with 1 µM PACAP(6-38) for 15 min blocked both PACAP-stimulated PAC1-EGFP receptor endocytosis and ERK activation (panels E and F). These results demonstrate that the PAC1 receptor antagonist can not only block PAC1 receptor cell surface-initiated signaling but also receptor endocytosis/trafficking and downstream endosomal signaling. Representative data from 3 separate culture wells. Scale bar = 10 µm.

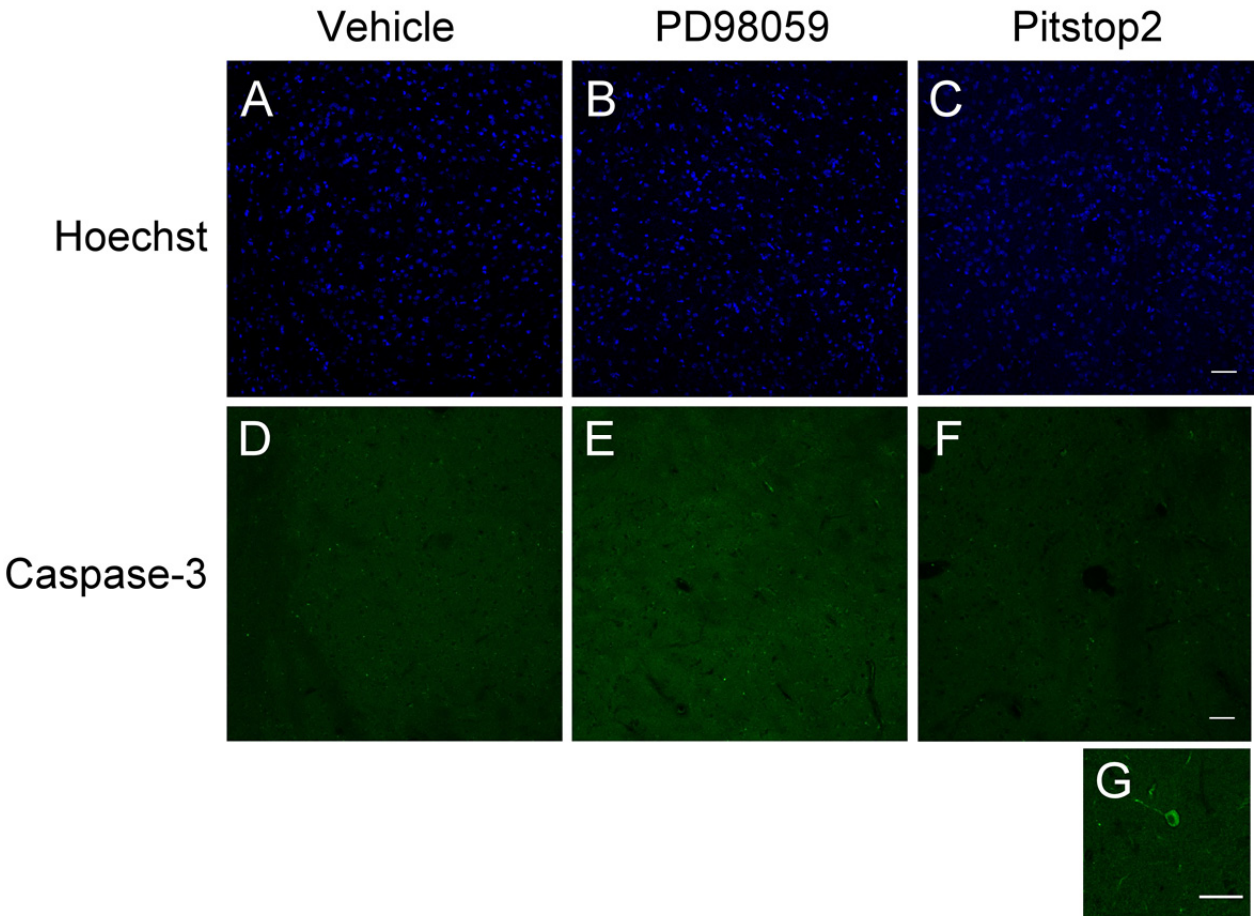


**Figure S10.** Acute CeA infusions with inhibitors do not induce apoptosis. To verify that the CeA infusions with drugs to block MEK (PD98059) or endocytic mechanisms (Pitstop 2) did not cause overt neurotoxicity and apoptosis to impact results, the treated tissues were also processed for nuclear Hoechst staining (A - C) and apoptotic marker cleaved caspase-3 immunoreactivity (D - F). Hoechst nuclear staining confirmed there were no apparent signs of substantial cell loss in any of the treatment conditions; further, there were no signs of any ongoing apoptosis in the CeA. Cleaved caspase $3^+$ cells were found sporadically throughout the brain; G, an example of a cleaved caspase $3^+$ hippocampal neuron shown at the same magnification. n = 7 - 8 animals per group. Scale bar = 50 µm.

## Supplemental References


1. Condro MC, Matynia A, Foster NN, Ago Y, Rajbhandari AK, Jayaram B, et al. (2016): High-resolution characterization of a PACAP-EGFP transgenic mouse model for mapping PACAP-expressing neurons. . *J Comp Neurol*. [Epub ahead of print] PMID: 27197019 .

2. Bennett GJ, Xie YK (1988): A peripheral mononeuropathy in rat that produces disorders of pain sensation like those seen in man. *Pain*. 33:87-107.

3. Missig G, Roman CW, Vizzard MA, Braas KM, Hammack SE, May V (2014): Parabrachial nucleus (PBn) pituitary adenylate cyclase activating polypeptide (PACAP) signaling in the amygdala: implication for the sensory and behavioral effects of pain. *Neuropharmacology*. 86:38-48.

4. Roman CW, Lezak KR, Hartsock MJ, Falls WA, Braas KM, Howard AB, et al. (2014): PAC1 receptor antagonism in the bed nucleus of the stria terminalis (BNST) attenuates the endocrine and behavioral consequences of chronic stress. *Psychoneuroendocrinology*. 47:151-165.

5. Hannibal J (2002): Pituitary adenylate cyclase activating peptide in the rat central nervous system: an immunohistochemical and in situ hybridization study. *J Comp Neurol*. 453:389-417.

6. May V, Buttolph TR, Girard BM, Clason TA, Parsons RL (2014): PACAP-induced ERK activation in HEK cells expressing PAC1 receptors involves both receptor internalization and PKC signaling. *Am J Physiol Cell Physiol*. 306:C1068-C1079.

7. May V, Lutz E, MacKenzie C, Schutz KC, Dozark K, Braas KM (2010): Pituitary adenylate cyclase-activating polypeptide (PACAP)/PAC1HOP1 receptor activation coordinates multiple neurotrophic signaling pathways: Akt activation through phosphatidylinositol 3-kinase and vesicle endocytosis for neuronal survival. *J Biol Chem*. 285:9749-9761.

8. Padgett CL, Lalive AL, Tan KR, Terunuma M, Munoz MB, Pangalos MN, et al. (2012): Methamphetamine-evoked depression of GABA(B) receptor signaling in GABA neurons of the VTA. *Neuron*. 73:978-989.

9. Tsuneoka Y, Maruyama T, Yoshida S, Nishimori K, Kato T, Numan M, et al. (2013): Functional, anatomical, and neurochemical differentiation of medial preoptic area subregions in relation to maternal behavior in the mouse. *J Comp Neurol*. 521:1633-1663.

10. Turner TN, Sharma K, Oh EC, Liu YP, Collins RL, Sosa MX, et al. (2015): Loss of δ-catenin function in severe autism. *Nature* 520:51-56.

11. Wake H, Ortiz FC, Woo DH, Lee PR, Angulo MC, Fields RD (2015): Nonsynaptic junctions on myelinating glia promote preferential myelination of electrically active axons. *Nature communications*. 6:7844.

12. Schneider CA, Rasband WS, Eliceiri KW (2012): NIH Image to ImageJ: 25 years of image analysis. *Nat Methods*. 9:671-675.

13. Braas KM, May V (1999): Pituitary adenylate cyclase-activating polypeptides directly stimulate sympathetic neuron neuropeptide Y release through PAC(1) receptor isoform activation of specific intracellular signaling pathways. *J Biol Chem*. 274:27702-27710.

14. Hammack SE, Cheung J, Rhodes KM, Schutz KC, Falls WA, Braas KM, et al. (2009): Chronic stress increases pituitary adenylate cyclase-activating peptide (PACAP) and brain-derived neurotrophic factor (BDNF) mRNA expression in the bed nucleus of the stria terminalis (BNST): roles for PACAP in anxiety-like behavior. *Psychoneuroendocrinology*. 34:833-843.

15. Amir-Zilberstein L, Blechman J, Sztainberg Y, Norton WH, Reuveny A, Borodovsky N, et al. (2012): Homeodomain protein otp and activity-dependent splicing modulate neuronal adaptation to stress. *Neuron*. 73:279-291.

16. Jean-Alphonse F, Hanyaloglu AC (2011): Regulation of GPCR signal networks via membrane trafficking. *Mol Cell Endocrinol*. 331:205-214.

17. Luttrell LM, Gesty-Palmer D (2010): Beyond desensitization: physiological relevance of arrestin-dependent signaling. *Pharmacol Rev*. 62:305-330.